

# PREPARATION OF POROUS CERAMIC BASED ON $\text{Al}_2\text{O}_3$ AS A RESULT OF ZONAL COMPACTION DURING SINTERING OF POWDER WORKPIECES OF VERY FINE ALUMINUM POWDER PAP-2 COMBUSTION PRODUCTS

D. A. Ivanov,<sup>1,4</sup> A. I. Sitnikov,<sup>2</sup> G. E. Val'yano,<sup>3</sup> T. I. Borodina,<sup>3</sup> and S. D. Shlyapin<sup>1</sup>

Translated from *Novye Ogneupory*, No. 9, pp. 28 – 34, September, 2018.

*Original article submitted May 24, 2018.*

Production aspects are considered for preparing porous ceramic based on  $\alpha\text{-Al}_2\text{O}_3$  using the effect of zonal compaction during powder workpiece sintering of very fine combustion products in air of flaky aluminum powder PAP-2 particles. It is shown that formation of a porous structure in sintered material proceeds by a local breakage mechanism through boundaries of aggregates with formation of pores between agglomerates, and also due to occurrence of a closed intergranular pore system. Properties of the ceramic obtained are: density 2.45 g/cm<sup>3</sup>, total porosity 39%, open porosity 30%, closed porosity 9%, the and ultimate strength in bending 50 – 60 MPa.

**Keywords:** porous aluminum oxide ceramics, aluminum powder PAP-2, filter combustion (FC), zonal compaction, inter-aggregate and intragranular pores.

## INTRODUCTION

Porous ceramic materials are in demand for use as effective high-temperature heat insulation in various heating units [1 – 6]. They are used extensively as filters, membranes, and catalyst carriers [7, 8]. This gives rise to development of new production approaches for creating these objects within which there is a combination of high porosity with a sufficient level of strength properties, and provision of prescribed thermophysical and operating properties (for example thermal conductivity, thermal shock resistance, corrosion resistance, and additional shrinkage).

It is very promising to prepare these materials using fine boehmite as a starting raw material, i.e., a product of hydrothermal synthesis of aluminum powder [7]. In this case possibilities are achieved of combining in the material nano-porosity and a nano-crystalline structure, which provide im-

provement of object strength. Formation of mesopores in ceramic has been recorded using finely dispersed carbon black as a burn-off addition [8]. In order to prepare porous permeable ceramic use of a strengthening binder is well known (very fine corundum powder, and also a mixture of very fine SiC and MgO powders), added to a powder mixture with special selection of grain size composition for the electro-melted corundum [0].

Previously we have demonstrated the possibility of an economic method for preparing porous heat resistant ceramic based on  $\text{Al}_2\text{O}_3$  of spherulitic structure and heat insulation from kaolin fibers using a filtration combustion (FC) method in air, or powder workpieces (PW) containing aluminum powder of commercial grade PAP-2 [10]. In this case aluminum powder fulfilled the function of a plastic binder and a component that on heating ignited a PW and occurrence of an exothermic aluminum combustion reaction within its volume. On FC completion there was PW sintering in air at 1500°C providing complete aluminum oxidation.

A production approach is proposed within the scope of the present work making it possible to form a porous structure within aluminum oxide ceramic due to implementing the effect of zonal compaction during powder workpiece sintering products of PAP-2 powder combustion in air.

<sup>1</sup> FGBOU Moscow Aviation Institute (National Research University), Moscow, Russia.

<sup>2</sup> FGBUN A. A. Baikov Institute of metallurgy and materials Science, Moscow, Russia.

<sup>3</sup> FGBUN Joint High-Temperature Institute, Russian Academy of Sciences, Moscow, Russia.

<sup>4</sup> dali\_88@mail.ru

## EXPERIMENTAL PROCEDURE AND RESEARCH

The starting raw material used was aluminum powder grade PAP-2 (GOST 5494) with flaky shape of particles of sub-micron thickness. Previously it was heated in air to 350°C and held for a time providing burn-off of stearin from the surface of particles and formation of a passivating aluminum oxide film replacing stearin. The powder obtained was charged into a refractory vessel heated in air at 500°C initiating combustion of its surface and subsequent combustion of the whole powder volume. The duration of combustion of a powder charges weighing 50 g was 10 – 15 sec, and the maximum combustion temperature was about 2000°C. After completion of combustion a sinter was formed, i.e., a product of rapid PAP-2 combustion. It was ground in a planetary mill using a drum vessel and spherical grinding bodies of corundum. Test specimens were compacted from the ground sinter under a pressure of 200 MPa and sintered in air at 1700°C for 2 h.

In addition, PAP-2 powder was heated in air by a regime (Fig. 1) providing slow oxidation in a flow regime in order to compare its final phase composition with that of the PAP-2 rapid combustion product. For this purpose a sample of PAP-2 ( $m_0 = 0.5145$  g) on an aluminum oxide substrate was placed in a muffle furnace and heated to a prescribed temperature  $T_{pre}$  (from 400 to 900°C with a step of 50°C) with subsequent isothermal exposure for 5 h. The overall duration of sample oxidation comprised 55 h.

The authors of the present article propose evaluating the thickness of an aluminum oxide film  $h$  on flaky particles after each heat treatment of a PAP-2 sample by calculation, using the following relations:

$$S_s = 0.5145 S_{sp} = m_0 S_{sp}, \quad (1)$$

where  $S_s$  is PAP-2 sample surface,  $m^2$ ;  $S_{sp}$  is PAP-2 specific surface,  $m^2/g$ ;  $S_{sp} = 4.1322$   $m^2/g$ ;

$$A = (m_i - m_0)/m_0 \times 100, \quad (2)$$

where  $A$  is relative weight increase for a PAP-2 sample after heat treatment in air at  $T_{pre}$ , %;  $m_i$  is current PAP-2 sample weight after heat treatment in air at  $T_{pre}$ ;

$$B = Am_0/100, \quad (3)$$

where  $B$  is the amount of oxide phase formed after heat treatment in air at  $T_{pre}$ , hg;

$$C = B/\rho, \quad (4)$$

where  $C$  is volume of oxide phase formed after heat treatment in air  $T_{pre}$ ,  $cm^3$ ;  $\rho$  is theoretical density of the  $\gamma$ - $Al_2O_3$  formed,  $g/cm^3$ ;  $\rho = 3.65$   $g/cm^3$ ;

$$h = C/S_s \times 10^3, \quad (5)$$

where  $h$  is aluminum oxide film thickness after each subsequent heat treatment in air, nm.

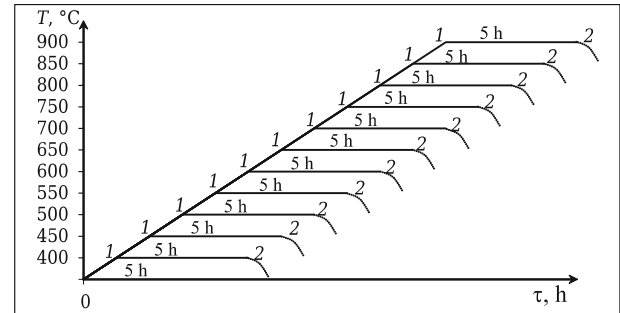


**Fig. 1.** Heat treatment regime for PAP-2 sample in air ( $T$  is prescribed temperature;  $\tau$  is time); 1 and 2) start and end of isothermal exposure respectively.

Then using the method of substitution of expression (1) – (4) in relationship (5) we obtain

$$h = [(m_i - m_0)/\rho m_0 S_{sp}] \times 10^3. \quad (6)$$

It should be noted that relationship (6) is rough since it does not take account of a possible change in PAP-2 specific surface as a result of heat treatment in air; some particle agglomeration is possible as a result of both sticking and as a result forming finely dispersed combustion products in a glow regime. In addition, the initial thickness of the passivating aluminum oxide film formed on PAP-2 particles of stearin burn-off was ignored, assuming that it is small and may comprise 0.5 – 1.0 nm [11].

X-ray phase analysis of materials was conducted in DRON-3 unit ( $Cu K_\alpha$  radiation) by a standard procedure, and local x-ray spectral analysis (EDX) and a study of the microstructure of specimen fractures were carried out in a Nova NanoSem 650 scanning electron microscope using an EDAX system. PAP-2 powder surface was determined by a procedure of low-temperature adsorption of nitrogen (BET) in a Micromeritics Tristar 3000 unit, ultimate strength in bending was determined for prismatic specimens with a size of  $8 \times 8 \times 50$  mm using a three-point loading scheme with a deformation rate of 1 mm/min in a Tiratest-2300 unit, and density, porosity and relative volume shrinkage of specimens were calculated by a generally accepted procedure [12].

## DISCUSSION OF RESULTS

### Features of slow PAP-2 powder oxidation in air in the range 400 – 900°C

It has been established that oxidation of PAP-2 particles in glow regime leads to formation at their surface of a  $\gamma$ - $Al_2O_3$  film on heating to a temperature below 900°C (see Table 1). With implementation of a regime  $T_{pre} = 900^\circ C$ ,  $\tau = 5$  h as a result of an increase in diffusion coefficient synthesis of multiphase oxide component is observed in surface films of aluminum particles and x-ray amorphous substance. In this case calculation of the integral density of multiphase

oxide component in these films becomes impossible due to the uncertain contribution of the x-ray amorphous substance on this property. Therefore, during calculation of oxide film thickness  $h$  using relationship (6) a value of  $\rho$  was conditionally adopted equal to 3.65 g/cm<sup>3</sup>. It should be noted that total oxidation of aluminum was attained on heating powder in air to 1630°C with subsequent isothermal exposure for 5 h (see Table 1).

Geometric interpretation of relationship (6) (Fig. 2) makes it possible to reveal some features of the oxidation of flat flaky PAP-2 particles. It is seen that an increase in  $h$  in the range 400 – 600°C is described by a saturation curve. Up to 600°C the increase in this parameter is “slowed down” by protective action of aluminum oxide films formed at the surface of flaky particles and preventing air oxygen diffusion towards aluminum. After exceeding the melting temperature  $T_m$  for aluminum the dependence of  $h$  on prescribed heat treatment temperature is linear in nature (an inflection is observed at a point corresponding to  $T_m$  for Al). In this case a dense aluminum oxide film maintains overheated ( $>T_m$ ) molten aluminum. In the range 600 – 900°C a uniform increase in  $h$  is observed due to an increase in gas permeability of aluminum oxide surface films in aluminum particles with an increase in temperature as a result of thermal expansion. It is probable that the yield of aluminum oxide phase in this case could increase significantly with occurrence of breaks in oxide films and emergence of melt at their surface. However, this process is prevented due to momentary passivation of melt by a new oxide film due to an exothermic reaction: aluminum (melt) + air oxygen (gas). It should be noted that the maximum value of  $h$  (47 nm) reached at 900°C, corresponds to the nano-range.

#### Features of PAP-2 powder oxidation by combustion in air (maximum brightness temperature ~2000°C)

A specific feature of this process is synthesis of a very small amount of a high-temperature modification of  $\alpha$ -Al<sub>2</sub>O<sub>3</sub> and formation of AlN and AlON as dominant phases, i.e., combustion products. The phase composition of sinter obtained as a result of combustion of PAP-2 powder in air (content of crystalline phase, %, in the numerator, average size of OCR, nm, in the denominator): AlN 41/100, AlON 28/44,

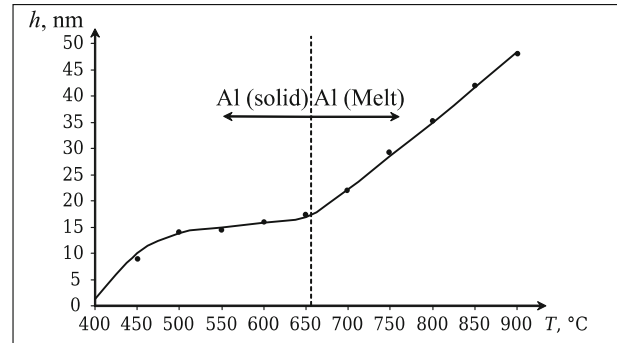


**Fig. 2.** Dependence of aluminum oxide film thickness  $h$  on flat flaky particles on prescribed heat treatment temperature  $T$  in air for a PAP-2 powder sample ( $\tau$  at each prescribed temperature 5 h).

$\alpha$ -Al<sub>2</sub>O<sub>3</sub> 2/10, Al 29/100. In this case retention of a significant proportion of unoxidized aluminum is recorded.

It may be suggested that rapid heating of PAP-2 aluminum powder to a significant temperature, reaching approximately  $3T_m$  for Al activates preferred reaction of flaky aluminum particles with nitrogen molecules adsorbed and held at its surface from a gaseous medium (N<sub>2</sub> + 2 – 8 vol.% O<sub>2</sub>) within which prolonged grinding of aluminum raw material in order to prepare powder was performed [13]. In this case the possibility should be considered of mechanical alloying of aluminum particles with nitrogen atoms as a result of prolonged impact-wear action of hard alloy grinding bodies, as a result of which there is introduction of nitrogen atoms into the aluminum crystal lattice. Then with high-temperature heating of PAP-2 to the maximum combustion temperature desorption of nitrogen molecules does not manage to occur and therefore preferred synthesis of AlN and AlON is initiated. In this case synthesis of these phases at a temperature exceeding  $T_m$  for Al will proceed due to reaction in the system gas (N<sub>2</sub>) – melt (al) within the volume of particles with protective action of oxide films holding melt. In this case as has been shown previously (see Table 1) with slow PAP-2 heating and prolonged isothermal exposure  $\tau$  formation of exceptionally modifications of Al<sub>2</sub>O<sub>3</sub> is observed, which points to occurrence of total desorption of nitrogen molecules at the surface of flaky particles under these conditions.

The composition of sinter formed after completion of PAP-2 combustion (Fig. 3a) is characterized by an extremely non-uniform structure. Formation of growths  $l$  of polyhedral particles is observed, whose transverse sizes comprise 60 – 70 nm (Fig. 3b). Formation of these nano-polyhedra is apparently explained by droplet formation from lumps of flaky particles and dust fraction of PAP-2 with rapid heating ( $>T_m$  for Al) with subsequent molten droplet reaction with gas phase and

**TABLE 1.** PAP-2 Powder Phase Composition in Relation to Heat Treatment Regime in Air

PAP-2 heat treatment regime	Crystal phase content, wt. %					X-ray-amorphous phase content, wt. %
	Al <sub>2</sub> O <sub>3</sub> *				Al	
	$\delta$	$\gamma$	$\theta$	$\alpha$		
650°C, 5 h	—	60/14	—	—	40/100	—
750°C, 5 h	—	76/10	—	—	24/100	—
900°C, 5 h	26/29	17/10	16/20	10/100	3/100	28
1630°C, 5 h	—	—	—	100/100	—	—

\* Crystal phase content in the numerator, average OCR size, nm, in the denominator.

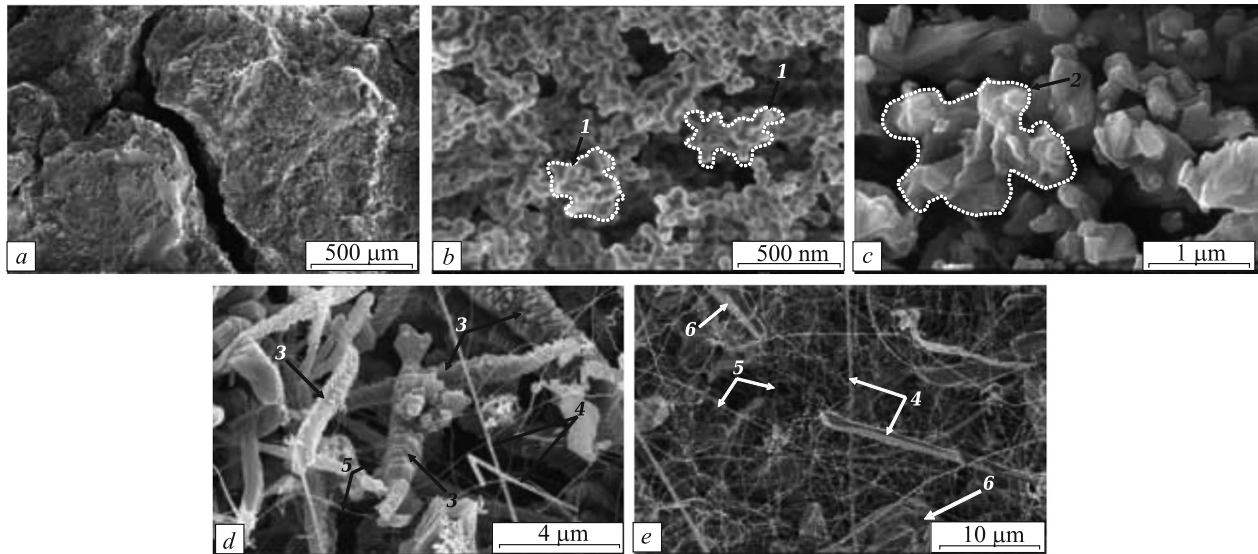


**Fig. 3.** Structure of sinter obtained as a result of burning PAP-2 powder in air: *a*) sinter general appearance; *b*) polyhedral particles within concretion composition 1; *c*) lamellae plates within the composition of isometric morphological object 2; *d*) lamellar particles within the composition of columnar morphological objects 3; 4 is acicular crystal; 5 is fine fibers; *e*) 4 is acicular crystals; 5 is fine fibers; 6 is lamellar particles.

crystallization. The structure of sinter is also represented by isometric 2 and columnar 3 morphological objects, consisting of lamellar particles (Fig. 3*c, d*). These particles inherit the shape of the flat PAP-2 flakes. In this case they acquire mainly tetragonal and hexagonal faceting as a result of rapid evaporation of aluminum from the edge of flakes and their rectilinear levelling, providing a minimum value of surface energy for the powder system in question. It should be noted that the volume of corundum columnar morphological objects lamellar particles were sintered over conjugated planes.

Within the structure of sinter there is also formation of acicular crystals 4 and thin fibers 5 (Fig. 3*d, e*). According to EDX data their elementary composition is represented by aluminum and nitrogen. This makes it possible to conclude that these structural elements consist of aluminum nitride. They probably arise by an evaporation-condensation mechanism, which is realized as follows: during combustion there is active evaporation of aluminum (as a rule as has been shown previously [14] Al vapor pressure during combustion in a given temperature range is quite high and comprises 245 to  $164 \times 10^2$  Pa). In this case aluminum vapor within the pore space of a PAP-2 powder charge reacts with nitrogen atoms that are gas components, i.e., a product of partial desorption of  $N_2$  from the surface of flaky aluminum particles. As a result of this gas phase reaction there is synthesis of AlN vapor that condenses within the volume of sinter in the form of acicular crystals and fine fibers during cooling [15, 16].

#### Sinter particle structure after grinding in a planetary mill

As a result of grinding sinter powder was obtained consisting of porous agglomerates 1 (Fig. 4*a*). Their dimensions

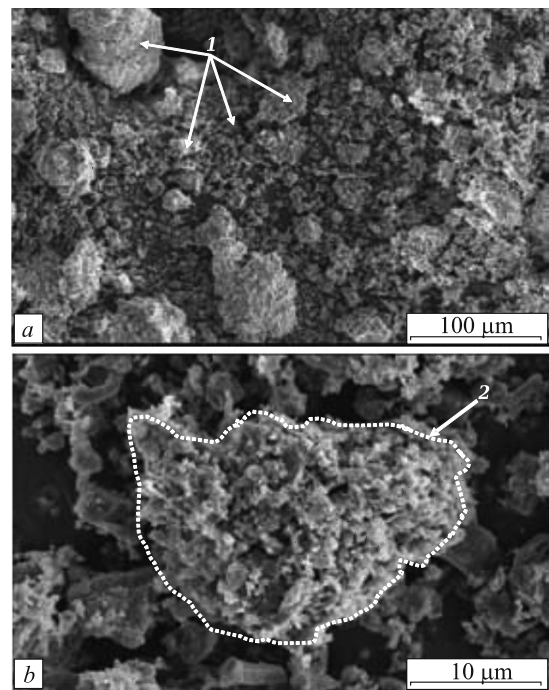


**Fig. 4.** Powder particles prepared as a result of refining sinter, i.e., product of PAP-2 powder combustion in air: *a*) porous agglomerates 1 (general appearance); *b*) agglomerate porous structure 2.

are predominantly in the range 5 – 100 μm. They form from nano-particles, which are a product of refinement of morphological objects present within the sinter composition. Among these particles of the nano-range dispersed forces operate, which determines the quite high strength of the agglomerates formed. An agglomerate pore structure is shown in Fig. 4*b*.

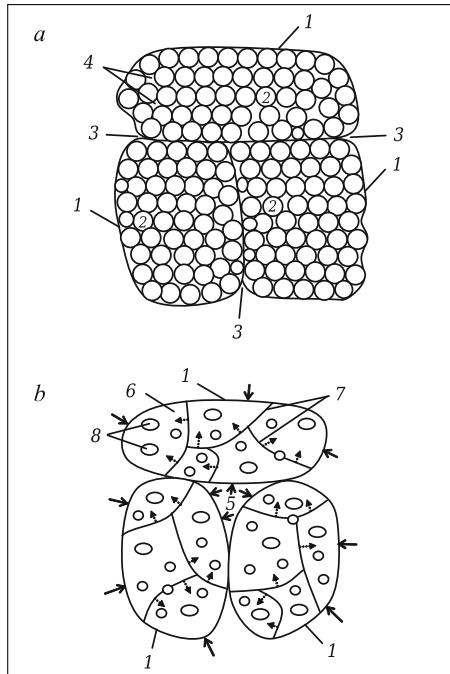


**Fig. 5.** Schematic image of zonal compaction processes during sintering a powder workpiece of nano-particles: *a*) raw material structure; *b*) sintered material structure; 1) agglomerates; 2) nano-particles; 3) boundaries between agglomerates; 4) intra-agglomerate pore; 5) inter-agglomerate pore; 6) grains; 7) intergranular boundary; 8) intergranular pores (arrows show direction of agglomerate 1 compression as a result of shrinkage and the direction of intergranular boundary migration 7 as a result of selective recrystallization).

It should be noted that retention within the sinter composition of a certain proportion of unoxidized aluminum, as shown above, makes it possible to compact the powder obtained without a temporary organic binder due to ductility of the metal component. In this case during refining sinter there is “smearing” of aluminum on the agglomerate surface.

#### Physicomechanical properties and features of sintered ceramic structure

The ceramic obtained is characterized by a combination of significant porosity (*P*) and relative volumetric shrinkage ( $\Delta V/V_0$ ) that is a feature of sintering nano-size powder systems, and is also has quite for very porous material ultimate strength in bending  $\sigma_{ben}$ . Ceramic density comprises 2.45 g/cm<sup>3</sup>, total, open, and closed *P* are correspondingly 39, 30, and 9%,  $\Delta V/V_0$  is 40%, and  $\sigma_{ben}$  is 50 – 60 MPa. The phase composition of an average powder sample prepared by grinding a sintered specimen is represented by the following crystalline phases, vol.%:  $\alpha$ -Al<sub>2</sub>O<sub>3</sub> 97, gibbsite Al<sub>2</sub>O<sub>3</sub>·3H<sub>2</sub>O 2.5, Al 0.5. The size of the OCR for these phases is 124 and 42 nm respectively. This phase composition points to complete thermal decomposition during sintering of nitride and oxynitride phases present within the original powder and

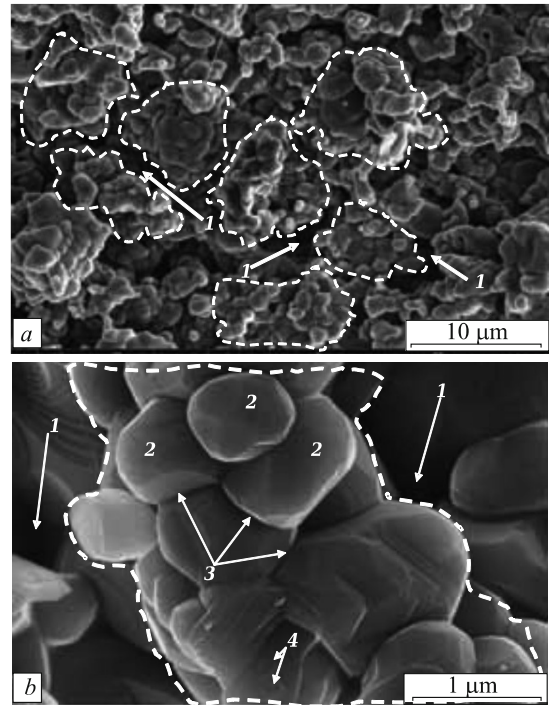


**Fig. 6.** Sintered aluminum oxide ceramic fracture surface: *a*) General view of material structure; 1) inter-agglomerate pores; *b*) agglomerate structure; 2) grains; 3) intergranular boundaries; 4) intra-granular pores.

$\alpha$ -Al<sub>2</sub>O<sub>3</sub> synthesis. Formation of gibbsite apparently proceed due to the extremely high activity a developed pore space in material with respect atmospheric air moisture in the cooling stage after sintering. It may also be suggested that presence of traces of aluminum in sintered ceramic are observed as a result of the protective action of an oxide phase preventing diffusion of oxygen atoms.

It has been established that a porous structure of material forms as a result of zonal compaction during sintering of the very fine nano-size powder system used (Fig. 5). Agglomerates 1, consisting of nano-particles 2, may be considered as areas within which density exceeds the local density of boundaries between agglomerates 3. Between nano-particles there are pores within agglomerates 4, whose size is comparable with that of nano-particles (see Fig. 5*a*). During sintering there is shrinkage, accompanied by compression of agglomerates (see Fig. 5*b*). In this case agglomerates are areas within whose volume there is predominantly compaction as a result of shrinkage (whence occurrence of the term “zonal compaction”). A result of zonal compaction is local separation over boundaries of neighboring agglomerates 1 in contact with formation of pores between agglomerates 5. In this case there is diffusion consolidation of particles with formation of grains 6, which determines the tendency of the system towards lower surface energy. In this case there is capture within the composition of grains 6 of pores within agglomerates that become pores between grains 7. Then as a re-

sult of migration of intergranular boundaries 8 due to selective recrystallization there is redistribution of the number of pores contained within a grain. In addition, with prolonged isothermal exposure coalescence might be expected. It should be noted that a system of pores between agglomerates within a specimen forms its open pore space structure and pores between grains are closed.

The sintering mechanism described above is confirmed by scanning electron microscopy data (Fig. 6). It is seen that the size of agglomerates in sintered material comprises 7–10  $\mu\text{m}$  (see Fig. 6a), the size of grains within the agglomerate composition is 0.5–1.5  $\mu\text{m}$ , and pores between grains 4 are nano-size (100–200 nm, see Fig. 8b). Analysis of aluminum oxide specimen surface fracture points to predominant failure by crack propagation through inter-granular and inter-agglomerate boundaries (see Fig. 6a, b). Failure is also observed by shear of individual grains, and in this case there is “open” nano-size pores between grains 4.

## CONCLUSION

Features have been considered for preparing porous aluminum oxide ceramic using the effect of zonal compaction during sintering of powder workpieces of highly dispersed combustion products in air of flaky PAP-2 aluminum powder particles (combustion duration of a powder charge weighing 50 g 10–15 sec, maximum combustion brightness temperature about 2000°C).

It has been established that as a result of combustion in air of PAP-2 particles synthesis is observed in a sintered form of a small amount of high-temperature modification of  $\alpha\text{-Al}_2\text{O}_3$  (2%), and formation of AlN (41%) and AlON (28%) as dominant phases with retention of a significant proportion of unoxidized aluminum (29%). Formation AlN and AlON in these conditions may be connected with interaction of flaky aluminum particles with nitrogen molecules from a gas a medium adsorbed and retained at their surface ( $\text{N}_2 + (2-8) \text{ vol.}\% \text{ O}_2$ ), in which prolonged grinding of aluminum raw material was performed for powder preparation.

It has been recorded that after completion of PAP-2 combustion in sinter formation of growths is observed with polyhedral particles with transverse size of 60–70 nm, isometric and columnar morphological objects, consisting of nanosize lamellar particles with tetragonal hexagonal facets, and also nanosize acicular crystals and fibers. Sinter ground in a planetary was represented by porous agglomerates (5–100  $\mu\text{m}$ ) consisting of nanosize particles connected by dispersion forces.

Powder workpieces sintered in air (1700°C, 2 h), prepared by compaction of porous agglomerates obtained, had a phase composition pointing to thermal decomposition of AlN and AlON present in the original powder and syntheses is  $\alpha\text{-Al}_2\text{O}_3$ . Traces of aluminum were retained due to the protective action of oxides phase within then ceramic composition. It has been shown that formation of a porous structure

in sintered material is realized by a local separation mechanism over agglomerate boundaries with formation of open inter-agglomerate pores, and also as a result of occurrence of close intra-granular pore systems.

The material obtained with a density of 2.4  $\text{g}/\text{cm}^3$  and total, open and closed porosity correspondingly 39, 30, and 9% respectively has quite high ultimate strength in bending (6–60 MPa).

*Research was conducted within the scope of the main part of state assignment for high schools No. 11.7568/2017/B4 using equipment of the resource center for collective usage “Aerospace materials and technology” MAI.*

*Microscope analysis was performed in OIVT RAN by a subsidy for fulfilling a state assignment in accordance with a program for RAN fundamental research (theme GR No. AAAAA-16-116051810082-7).*

## REFERENCES

1. S. A. Glazyrin, R. A. Anakashev, N. G. Valiev, et al., “Heat insulation refractory coating,” Proc. Internat. Conf. of Refractory Workers and Metallurgists (6–7 April, 2017, Moscow), *Novye Ogneupory*, No. 3, 39 (2017).
2. R. V. Zubashchenko, “Study of the heat resistance of high-alumina heat insulation objects based on aluminum silicate fiber,” Proc. Internat. Conf. of Refractory Workers and Metallurgists (6–7 April, 2017, Moscow) *Novye Ogneupory*, No. 3, 42 (2017).
3. V. V. Martynenko, N. M. Kaznacheeva, Yu. A. Krakhmal', and K. I. Kushchenko, “Corundum lightweight refractories with improved thermotechnical properties,” Proc. Internat. Conf. of Refractory Workers and Metallurgists (6–7 April, 2017, Moscow). *Novye Ogneupory*, No. 3, 47–48 (2017).
4. V. N. Sokov, “Corundum spherical fillers with a broad range of grain size and different porous structure,” Proc. Internat. Conf. of Refractory Workers and Metallurgists (6–7 April, 2017, Moscow). *Novye Ogneupory*, No. 3, 53–54 (2017).
5. E. N. Demin and A. A. Rechkalov, “High-temperature monolithic foam insulation,” Proc. Internat. Conf. of Refractory Workers and Metallurgists (6–7 April, 2017, Moscow), *Novye Ogneupory*, No. 3, 69 (2017).
6. R. V. Zabushchenko and V. I. Kuzin, “Experience of using high-temperature insulation objects produced by ZAO PKF NK in heating unit lining,” Proc. Internat. Conf. of Refractory Workers and Metallurgists (6–7 April, 2017, Moscow), *Novye Ogneupory*, No. 3, 69–70 (2017).
7. A. V. Bersh, A. V. Belyakov, D. Yu. Mazalov, et al., “Formation and sintering of boehmite and aluminum oxide nanopowders,” *Refract. Indust. Ceram.*, **57**(6), 655–660 (2017).
8. A. Mocciano, M. B. Lombardi, and A. N. Scian, “Ceramic material porous structure prepared using pore-forming additives,” *Refract. Indust. Ceram.*, **58**(1), 65–68 (2017).
9. A. V. Belyakov, Zaw Ye Maw Oo, N. A. Popova, et al., “Strengthening binders for porous permeable ceramic with electromelted corundum filler,” *Refract. Indust. Ceram.*, **58**(1), 89–93 (2017).

10. D. A. Ivanov, S. D. Shlyapin, G. E. Val'yano, and L. V. Fedorova, "Structure and physicochemical properties of porous ceramic based on  $\text{Al}_2\text{O}_3$  prepared using a filtration method," *Refract. Indust. Ceram.*, **58**(5), 538 – 541 (2018).
11. P. F. Pokhil, A. F. Belyaev, Yu. V. Frolov, et. al., *Powder Metal Combustion in Active Media* [in Russian], Nauka, Moscow (1972).
12. N. T. Andrianov, A. V. Belyakov, A. S. Vlasov, et al., *Ceramic Technology Course: High School Textbook* [in Russian], Stroimaterialy, Moscow (2005).
13. V. G. Gopienko, M. G. Smagorinskii, A. A. Grigor'ev, and A. D. Belavin, *Aluminum Powder Sintered Materials*, [in Russian], Metallurgiya, Moscow (1993).
14. D. A. Ivanov, A. N. Simnikov, G. E. Val'yano, and S. D. Shlyapin, "Study of finely crystalline aluminum oxide coating on aluminum powder surface prepared as a result of filtration combustion," *Novye Ogneupory*, No. 1, 43 – 48 (2018).
15. D. A. Ivanov, A. I. Sitnikov, and S. D. Shlyapin, *Precipitation-Hardened Fiber and Layered Inorganic Composite Materials* [in Russian], MGIU, Moscow (2010).
16. E. I. Givarkizov, *Fiber and Lamellar Crystals Grown from Vapor* [in Russian], Nauka, Moscow (1977).